Polymer 50 (2009) 4868–4875

Contents lists available at ScienceDirect

Polymer

journal homepage: www.elsevier.com/locate/polymer

Glass transition behavior of hyper-branched polystyrenes

Kei-ichi Akabori [a], Hironori Atarashi [a], Masaaki Ozawa [b], Tetsuo Kondo [c], Toshihiko Nagamura [a], Keiji Tanaka [a,*]

[a] Department of Applied Chemistry, Kyushu University, 744 Motooka, Nishi-ku, Fukuoka 819-0395, Japan
[b] Nissan Chemical Industries Ltd., 722-1 Tsuboi-cho, Funabashi 274-8507, Japan
[c] Bio-Architecture Center, Kyushu University, 6-10-1 Hakozaki, Higashi-ku, Fukuoka 812-8581, Japan

ARTICLE INFO

Article history:
Received 25 April 2009
Received in revised form
10 August 2009
Accepted 18 August 2009
Available online 22 August 2009

Keywords:
Hyper-branched polymers
Glass transition
Fragility index

ABSTRACT

Hyper-branched polystyrenes (HBPS) were synthesized. The bulk glass transition temperature (T_g) measured by differential scanning calorimetry (DSC) for two kinds of HBPS with an equivalent M_w, which were fractionated from different lots, were different, being respectively higher and lower than that of the corresponding linear polystyrene (PS). Infrared spectroscopy revealed that the T_g of HBPS increased with an increasing extent of intramolecular cross-linking, or cyclization, in the molecule. The segmental dynamics of HBPS was examined by dynamic mechanical analysis. The relaxation temperature for the segmental motion in HBPS was consistent with the DSC results. The fragility index was always lower for HBPS than for the linear PS, regardless of its primary structure and chain end chemistry. This would indicate that the segmental motion for HBPS is less cooperative than that of the linear PS, probably due to a lack of intermolecular chain entanglements in HBPS.

1. Introduction

For the last two decades, dendritic polymers have been widely studied as a novel pathway to enhance synthetic polymer functions in the fields of coatings, drug delivery systems, supramolecular chemistry, nanotechnology, etc [1–15]. The most intriguing feature of dendritic polymers seems to be their versatility in introducing functional groups into end groups and the central part, termed the focal point, of a molecule. While a linear polymer has only two end groups, a dendritic polymer possesses $(n+1)$ ends, where n denotes the number of branching points in the molecule. This feature means that the number of chain ends for a dendritic polymer increases with increasing molecular weight. Thus, dendritic polymers have a tremendous potential as highly-functionalized materials due to the large number of chain ends acting as a functional moiety.

Dendritic polymers can be roughly categorized into two groups: dendrimers including dendrons and hyper-branched polymers (HBP) [16–18]. Dendrimers are synthesized by either a divergent or convergent method, and thus, the primary structure is thought to be well-defined, resulting in an almost perfectly monodispersed product. The glass transition temperatures (T_g) of dendrimers have been extensively studied [19–24]. One of the main conclusions obtained thus far is that T_g is sensitive to the generation number, namely, molecular weight as well as chain end chemistry. This point is extremely important in developing a clear relationship between the primary structure of polymers and T_g. However, since the synthesis of dendrimers with higher generations is quite complicated and difficult, they are not necessarily suitable for mass consumption in industrial fields except for a few kinds, such as poly(amidoamine) [1]. On the other hand, the synthetic routes for HBP are generally based on radical reactions, and so, are easier than that for dendrimers. Thus, to this date, various types of HBP have been synthesized, efforts that have led to a broad array of applications both in academic and industry. A disadvantage of HBP is that the primary structure is not clear, so that complications arise in understanding its physical properties. The T_g for HBPs with a wide range of monomer structures has hitherto been examined by differential scanning calorimetry (DSC) [25–40]. However, most studies focused on just the T_g values for products, which were not fractionated, and did not discuss the segmental dynamics.

Flory theoretically argued that the molecular weight distribution of HBP increases with increasing molecular weight [41]. This conclusion rests on the fact that HBP molecules with different degrees of branching are mixed in the product. Hence, as long as a non-fractionated HBP is used, the details of its glass transition behavior would essentially remain undetermined on account of its broad molecular weight distribution, resulting, in turn, in a broad T_g

* Corresponding author. Tel.: +81 92 802 2879; fax: +81 92 802 2880.
E-mail address: k-tanaka@cstf.kyushu-u.ac.jp (K. Tanaka).

0032-3861/$ – see front matter © 2009 Elsevier Ltd. All rights reserved.
doi:10.1016/j.polymer.2009.08.029

distribution. This difficulty motivated us to fractionate HBP samples for T_g measurements by DSC. In fact, we will present an interesting result showing that samples with equivalent molecular weights fractionated from different lots exhibit different T_gs.

In this study, the glass transition temperature and segmental dynamics of hyper-branched polystyrene (HBPS) were studied by DSC in conjunction with dynamic mechanical analysis (DMA). Our choice of the polystyrene (PS) backbone is based simply on the fact that the glass transition temperature and dynamics for the corresponding linear PS are well understood. Comparing the results for HBPS with our knowledge obtained by means of the linear PS, we discussed the effects on that compound of its unique architecture, branching structure, and chain end chemistry on its glass transition behavior.

2. Experimental section

The HBPS with dithiocarbamate end groups (HBPS–DC) were synthesized by a self-addition free radical photo-polymerization of *N*,*N*-diethylaminodithiocarbamoylmethylstyrene (DTCS) [42]. The HBPS with hydrogen termini (HBPS-H) were prepared by substituting HBPS–DC with a H-containing tin agent. Fig. 1 represents the synthetic route for HBPS–DC and HBPS-H. The photo-polymerization of DTCS in toluene solutions was carried out in a sealed glass vessel under UV irradiation at 303 K for 6 h. Then, the reduction of HBPS–DC to HBPS-H was induced at 303 K for 2 h by adding an excess amount of tributyltin hydride (Bu_3SnH) into a toluene solution of HBPS–DC. For comparison, linear polystyrene (PS) synthesized by a living anionic polymerization and linear PS having DC groups at every repeating unit (PS–DC) synthesized by a conventional radical polymerization of DTCS were also used.

The product obtained after the reduction reaction possessed a broad molecular weight distribution (M_w/M_n), where M_n and M_w denote number- and weight-average molecular weights. Table 1 summarizes the characterizations of samples used in this study. Here, the indexes of *l* and *h* in front of PS and HBPS-H stand for lower and higher M_w, respectively. The values of M_w and M_w/M_n were, respectively, determined by multi-angle laser light scattering (MALLS, DAWN HELEOS; Wyatt Technology Co. Ltd.) measurement and gel permeation chromatography (GPC, HLC-8120GPC; Tosoh Co. Ltd.) with a Shodex KF-804L column using PS standards. Both *l*HBPS-H and *h*HBPS-H were fractionated by GPC as a function of hydrodynamic volume. M_w and M_w/M_n values for the fractionated HBPS are tabulated in Table 2. The fractionated samples were used for T_g measurements. The T_g of the bulk samples was measured by DSC (Diamond DSC; PerkinElmer Co. Ltd.) with a power compensation type of scan at a cooling rate of 10 K min^{-1}. The T_g for HBPS-H was also predicted by PolyInfo [43] on the basis of van Krevelen's structural group contribution theory [44]. In PolyInfo, a repeating unit could not be too large, and thus, a unit containing three branching points was used for the prediction.

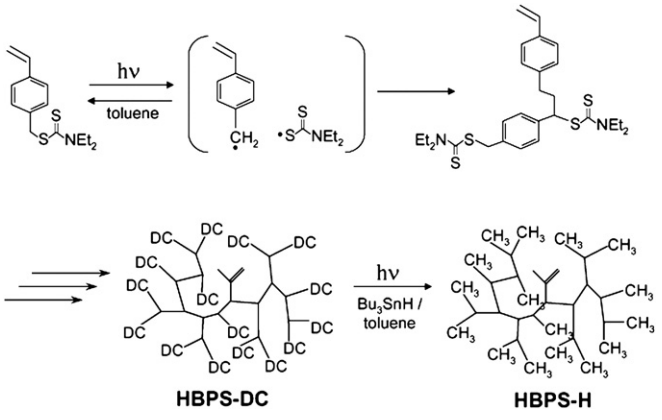

Fig. 1. Synthetic route for HBPS–DC and HBPS-H.

Table 1
Characterization of samples used in this study.

Sample	M_w	M_w/M_n	T_g/K
*l*HBPS-H	47 k	4.22	364
*l*PS	58 k	1.06	375
*h*HBPS-H	157 k	5.81	376
*h*PS	115 k	1.08	375
HBPS–DC	57 k	3.88	335
PS–DC	52 k	2.48	340

The extent of intramolecular cross-linking, or cyclization, for HBPS was examined by Fourier transform infrared (FT/IR) spectroscopy using a KBr pellet technique. The spectra were recorded at a resolution of 0.5 cm^{-1} with a Herschel FT/IR-620 spectrometer (JASCO Co. Ltd.); 512 scans were necessary to obtain spectra with a high signal-to-noise ratio. No signatures for the presence of crystals were observed on IR spectra and DSC charts for HBPS synthesized by a radical polymerization due to the atactic monomer sequences. Degree of branching [45,46], which was determined by ^{1}H NMR measurements, was ranging from 0.20 to 0.22 for HBPS–DCs used [47]. This value is in good accordance with the reported one for the same polymerization system estimated by a kinetic approach [48].

The thermal molecular motion of HBPS-H in films was examined by DMA (Rheovibron DDV-01FP, A&D Co., Ltd.). Self-supported films of HBPS-H could not be prepared due to a lack of intermolecular entanglements. Thus, a unique method for the measurements was used in this study. First, HBPS-H films with thickness of ca. 300 nm were prepared by a spin-coating method from toluene solutions onto a substrate of 7.5 μm-thick polyimide (PI) films [49]; then, they were annealed at a temperature above the T_g under 10^{-3} Torr for 24 h. After the annealing, the films were cooled at a rate of 0.5 K min^{-1}. Specimens with a width of 3 mm and a length of 30 mm were cut from the films thus prepared. The measurements were carried out at a heating rate of 1 K min^{-1} at a frequency ranging from 0.05 to 110 Hz, under a dry nitrogen purge. To realize such a wide frequency range, four independent measurements for specimens at a different set of frequencies were made. Beforehand, it was confirmed that the PI substrates did not exhibit a clear relaxation process in the temperature range of 300–400 K [49].

3. Results and discussion

3.1. The effects of molecular weight and chain end chemistry on T_g

As stated above, it has been reported that the T_g of HBP depends on both molecular weight and chain end chemistry [25–40]. Thus,

Table 2
M_w and M_w/M_n values for samples fractionated by GPC.

From *l*HBPS-H			From *h*HBPS-H			From HBPS–DC		
No.	M_w	M_w/M_n	No.	M_w	M_w/M_n	No.	M_w	M_w/M_n
1	19 k	1.29	1	14 k	1.28	1	51 k	1.34
2	29 k	1.25	2	23 k	1.24	2	77 k	1.18
3	47 k	1.22	3	69 k	1.19	3	95 k	1.19
4	61 k	1.20	4	116 k	1.14	4	127 k	1.18
5	80 k	1.16	5	194 k	1.19	–	–	–
–	–	–	6	441 k	1.14	–	–	–

we first discuss these issues using our samples. Fig. 2 shows the M_w dependence of T_g for our HBPS and PS samples. The T_g was determined to be the midpoint of the baseline shift on the plot of temperature vs. heat capacity during the cooling process. The data sets marked by filled circles and triangles were from samples fractionated from *l*HBPS-H and *h*HBPS-H, respectively. As shown in Table 2, the molecular weight distribution of each sample improved upon those of the original. The upper limit of the M_w for samples fractionated from *l*HBPS-H was 8×10^4, because that compound did not contain higher M_w fractions. Similarly, samples of HBPS–DC were also fractionated from a sample with an M_w of 57 k and M_w/M_n of 3.88.

First, we discuss the chain end effect on the T_g. The T_g values for the linear PS–DC were lower than those for the linear PS with an equivalent M_w by approximately 30 K. In addition, the T_g for the HBPS–DC was much lower than that for the HBPS-H. This is a clear indication that, as previously reported [25–40], chain end chemistry is one of the factors responsible for variations in T_g values, even for HBP. However, the T_g for the HBPS–DC was comparable to those for the linear PS–DC. Thus, it seems likely that, in the case of HBPS terminated with DC groups, the effect of large number density of DC groups on the T_g is much stronger than the effect of the architecture, so that no clear difference in the T_g exists between HBPS–DC and linear PS–DC.

In general, the T_g for polymers decreases with decreasing M_w values. This trend is simply expressed by the traditional Fox and Flory theory, where an extra free volume is induced by chain end portions [50]. After a slight modification, the equation can be applied even to HBP, as follows [21];

$$T_g = T_g^{\infty} - K'(n_e/M_w) \quad (1)$$

where n_e and K' are, respectively, the number of chain ends per molecule, and a constant related to the characteristics of a polymer. In Fig. 2, we plot the fitted data for HBPS-H and linear PS. In the case of linear PS, the fitting parameter of K' with a n_e of 2 was estimated to be about 5×10^4, a value is in good agreement with the reported one [50]. Given that the K' is related only to the free volume induced by the chain ends, the value should be invariant, regardless of the branching structure. If that is the case, the n_e values for HBPS-H are estimated to be 4.4 and 3.9, from *l*HBPS-H and *h*HBPS-H, respectively. However, taking into account the chemical structure of HBPS-H and M_w, these n_e values are judged to be unrealistic. Thus, the M_w dependence of T_g for HBP cannot be simply explained in terms of the chain end effect, strongly suggesting the contribution of the other factors.

When the M_w for linear polymers increases, T_g reaches a constant value, denoted as T_g^{∞}, because the number density of chain ends becomes smaller as the M_w values rise. This is the essence of the Fox–Flory theory. The T_g values for HBPS-Hs, taken from those for *l*HBPS-H and *h*HBPS-H, also reach constant values, 367 K and 382 K, at a semi-infinite M_w. However, the origin of the T_g^{∞} for HBP should be different from that for the linear polymers. According to Stutz's theoretical claim, the T_g for dendrimers depends on the end group conversion and the degree of branching [23]. In dendritic polymers, the branching portion would restrict thermal molecular motion occurring on a relatively large scale, such as segmental motion [23], an inhibition resulting in a T_g higher than that of the corresponding linear polymer [34]. Although the fraction of end groups and branching per molecule initially increase with increasing M_w, they quickly approach their limits at about the fourth or fifth generation, so that no M_w dependence of the T_g exists in a higher generation. Assuming that this notion is also applicable to HBP, we can clarify the invariance of T_g with M_w, as shown in Fig. 2.

3.2. The role of intramolecular cross-linking on T_g

The T_g for HBPS-H, taken from *h*HBPS-H, was higher than that from *l*HBPS-H at any given M_w in the entire range. The T_g difference at a specific M_w for the two kinds of HBPS-H, fractionated from different lots, could hardly be explained at first glance. A possible explanation for this variation is that molecular structure of *l*HBPS-H and *h*HBPS-H differs. As shown in Fig. 1, HBPS-H was obtained by reducing HBPS–DC. If *l*HBPS-H and *h*HBPS-H possess different primary structure, the original HBPS–DCs should also be structurally different from each other. Thus, FT-IR measurement was applied to the HBPS–DC with lower and higher molecular weights.

Fig. 3 shows the IR spectra for these samples in the wavenumber range from 1470 to 1520 cm^{-1}. For comparison, the spectrum for the linear PS–DC is also shown. Since all the spectra were normalized with the internal standard peak at 1510 cm^{-1} [51–53], corresponding to the C–C stretching vibration of aromatic rings, they can be directly compared to one another. The absorption band at 1485 cm^{-1} corresponds to the C–N stretching vibration of DC groups [54]. It is clear that the peak at 1485 cm^{-1} became smaller for HBPS–DC than for PS–DC. In addition, the decrement was more striking for the higher M_w HBPS–DC than for the lower one. If only

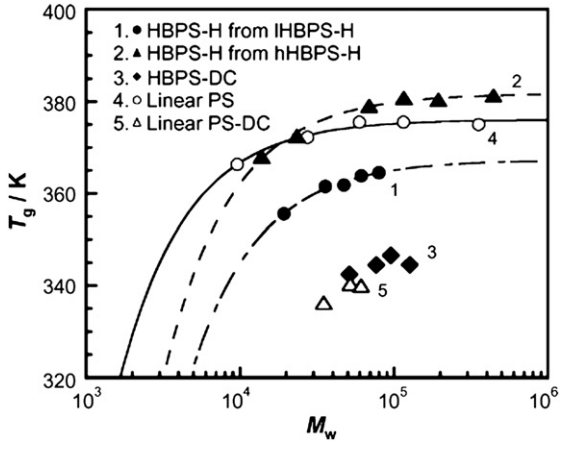

Fig. 2. M_w dependence of T_g for HBPS-H and HBPS–DC. Two kinds of HBPS-H fractionated from *l*HBPS-H and *h*HBPS-H were used. *l*HBPS-H and *h*HBPS-H possessed different M_w and M_w/M_n. For comparison, the data for linear PS and PS–DC are also shown.

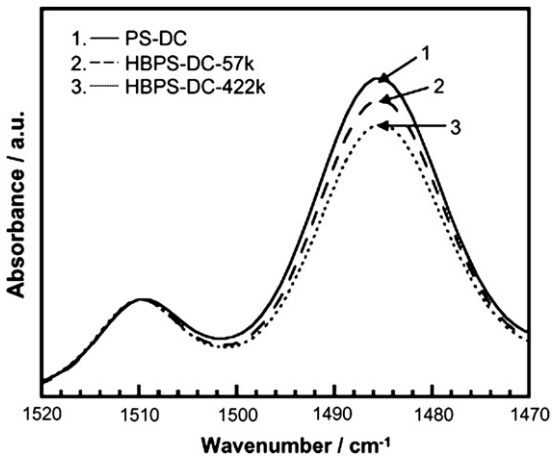

Fig. 3. IR spectra for PS–DC and HBPS–DC with different M_w. All the spectra were normalized with the internal standard at 1510 cm^{-1}.

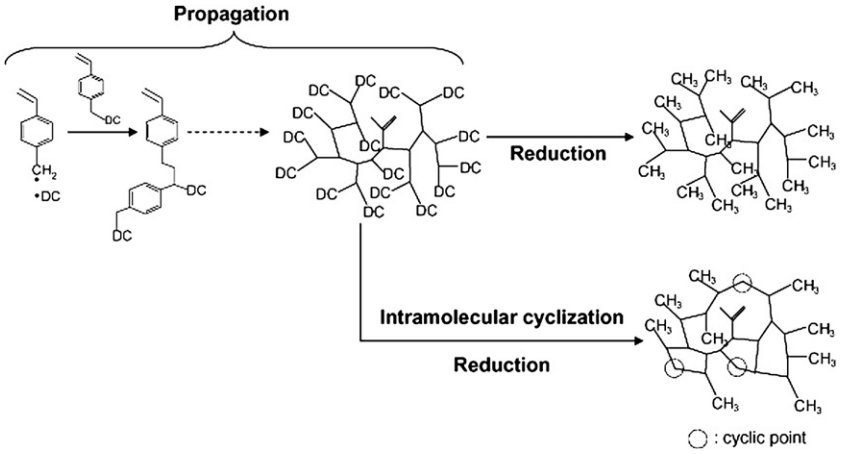

Fig. 4. Schematic representation of possible reactions in synthesis of HBPS under photo-irradiation.

the propagation reaction is occurred during the polymerization, the fractional amount of DC groups to aromatic rings should be invariant with respect to the branching structure. However, this was not the case in Fig. 3. Thus, it is most likely that some side reactions in addition to the propagation occurred and that the extent was more remarkable for the higher M_w HBPS–DC.

The most plausible side reaction is a recombination between radicals originated from DC groups, that is, intramolecular cyclization, which would make the molecule rigid, as the origin for this T_g difference. Of course, intermolecular cross-linking might also occur. However, if that effect was important, the substance would not dissolve in any solvent. Thus, the effect of intermolecular cross-linking can be excluded from the current discussion. Fig. 4 illustrates possible reactions during the photo-polymerization process of HBPS. There are two types of reactions: an addition of a radical species to a monomer and a recombination between radical species. The former is the propagation process in the polymerization, and produces the branching structure, either (CH_2CH_2CH) or ($CHCH_2CH$) unit between the nearest two phenyl rings. The sequential difference is based on the type of propagating radical, such as primary benzyl radical or secondary phenetyl one [55]. Then, the successive reduction incorporates methyl groups at end portions. On the other hand, the latter recombination reaction occurs during the photo-polymerization and/or the reduction. This generates intramolecular cyclic structure with any of (CHCH), (CH_2CH) or (CH_2CH_2) unit between the nearest two phenyl rings. Also, the number of end portions in a molecule is inversely proportional to the number of cyclic structure. Thus, products with a larger number of intramolecular cyclization should be more rigid due to their smaller number of carbons between the nearest two phenyl rings and smaller number of chain ends in addition to the presence of the cyclic structure itself. These factors should result in a higher T_g.

If the above-mentioned discussion is correct, the HBPS-H taken from the *h*HBPS-H, which exhibits a higher T_g than that from *l*HBPS-H, should have a larger number of intramolecular cyclic structures. To confirm whether this hypothesis is plausible, we also made IR measurements on two kinds of HBPS-H samples. Since DC groups are not existed in HBPS-H, other characteristic bands were used to judge the difference in their primary structures. Fig. 5 shows typical IR spectra within the wavenumber range from 2800 to 3200 cm^{-1} for two kinds of HBPS-H with a similar range of hydrodynamic volumes, fractionated from *l*HBPS-H and *h*HBPS-H [56]. Both spectra were again normalized using an absorption peak at 1510 cm^{-1} as an internal standard [51–53]. The absorption peaks observed at wavenumbers higher than 3000 cm^{-1} considerably overlapped each other, whereas the peaks observed at 2800–3000 cm^{-1} were separated. The former can be assigned to the C–H stretching vibration of aromatic rings [51–53], suggesting that the fractional amount and the chemical state of the phenyl groups are both independent of the branching structure. The absorption peaks at 2850 and 2920 cm^{-1} are assignable to the symmetric and anti-symmetric C–H stretching vibrations of methylene groups [51–53]. They became smaller for *h*HBPS-H than for *l*HBPS-H, a result suggesting that the methylene content per molecule is lower for *h*HBPS-H than for *l*HBPS-H. To further discuss the difference in the two spectra, the differential spectrum, subtracting *h*HBPS-H spectrum from the *l*HBPS-H one,

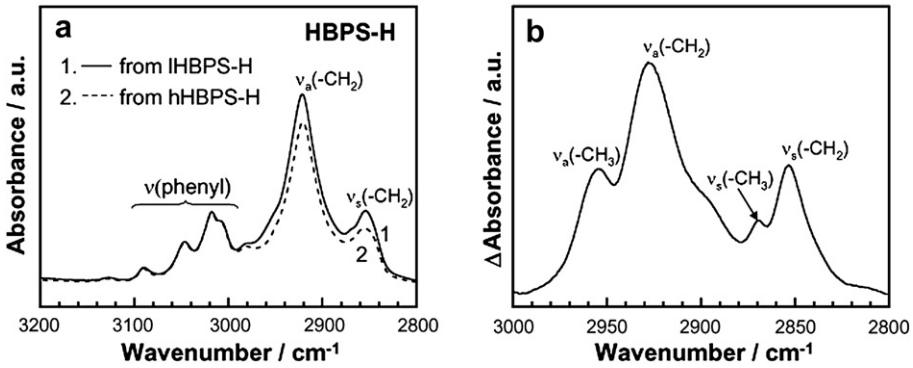

Fig. 5. (a) IR spectra for two kinds of HBPS-H fractionated from *l*HBPS-H and *h*HBPS-H. The differential spectrum between the two is plotted in the panel (b).

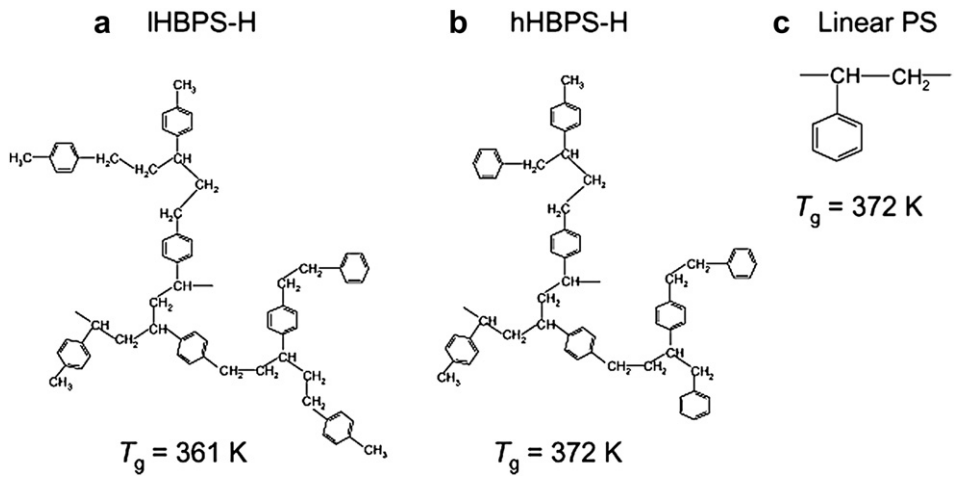

Fig. 6. T_g prediction for realistic, simplified model HBPS-Hs on the basis of van Krevelen's structural group contribution theory. For comparison, the prediction was also made for linear PS.

is shown in Fig. 5(b). On this figure, additional peaks appeared at 2870 and 2960 cm^{-1}, were assigned to the symmetric and anti-symmetric C–H stretching vibrations of methyl groups [51–53]. This means that the *l*HBPS-H possesses more methyl end groups than the *h*HBPS-H. Thus, it is evident why the series of HBPS-H from *h*HBPS-H exhibit a higher T_g than that from *l*HBPS-H: the former series contains more intramolecular cyclic portions.

3.3. Theoretical prediction of T_g

To confirm the effect of molecular structure on the T_g of HBPS, we adopted a method proposed by van Krevelen [44]. Since this method is based on structural group contributions, it should be noted that the cyclization effect on T_g is not included. However, once an intramolecular cyclic structure is formed rather than a propagation reaction proceeding, the chemical structure of a molecule is changed, as discussed after Fig. 4. In such a case, van Krevelen's method would still be qualitatively effective for our purpose. Fig. 6 shows the structures of HBPS-H and linear PS, and the T_g values predicted by the method. Due to calculation limits, only three branching points were incorporated into the construction of a HBPS-H molecule. The structural discrepancy between *l*HBPS-H and *h*HBPS-H was expressed by different sequences of methylene units, which were sandwiched between the aromatic rings, and the number of methyl end portions [57]. The T_g value for linear PS was calculated to be 372 K, which was quite reasonable. When the branching points were incorporated into the molecule, as shown in panel (a), the T_g decreased to 361 K. This value was consistent with the experimental T_g for HBPS-H with M_w of 30 k, and fractionated from *l*HBPS-H, as shown in Fig. 2. In the case of the model *h*HBPS-H depicted in panel (b), the T_g was higher than that for (a) by 11 K. Although the predicted T_g increment for *h*HBPS-H compared with *l*HBPS-H was slightly smaller than that seen in the experiment in Fig. 2, it is acceptable. The T_g predictions by van Krevelen's method reveal that the incorporation of C–C sequences instead of C–C–C ones, which are necessarily introduced by the intramolecular cyclization, makes the main chain rigid. Finally, we consider the origin of the underestimated T_g increment for *h*HBPS-H. As stated before, van Krevelen's method does not include the effect of cyclization. Thus, it seems most likely that the underestimation of the T_g increment for *h*HBPS-H arises from ignorance of the cyclization effect.

3.4. Relationship of T_g to the degree of cross-linking

To examine to what extent T_g increases with the progress of the recombination reaction, that is, a cross-linking, HBPS–DC was annealed at 423 K, with or without photo-irradiation, and then T_g for the products was measured. Actually, the cross-linking effect on T_g should be studied using HBPS-H. However, after annealing, HBPS–DC would not dissolve in any organic solvents due to the presence of intermolecular cross-linking, making it impossible to complete the reduction reaction to HBPS-H. Thus, this discussion centers on HBPS–DC instead. Fig. 7(a) shows the annealing time dependence of the T_g increment, with and without UV irradiation. The ΔT_g ordinate is defined as the difference in T_g between the

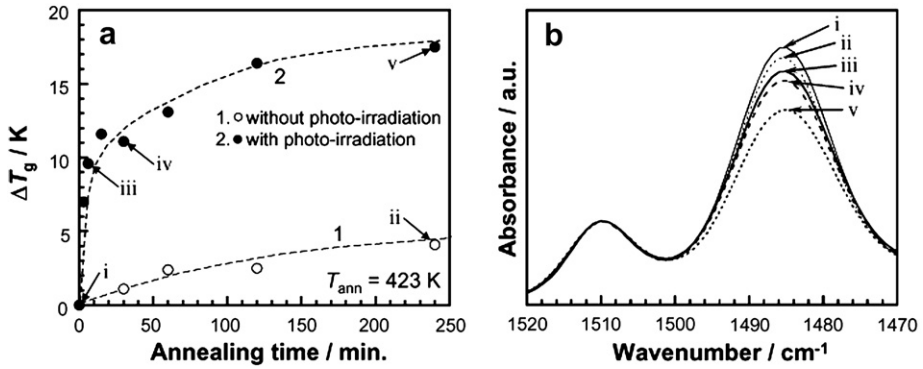

Fig. 7. (a) Annealing time dependence of T_g increment for HBPS–DC at 423 K with and without UV irradiation. (b) IR spectra for HBPS–DC marked by arrows with i–v in the panel (a).

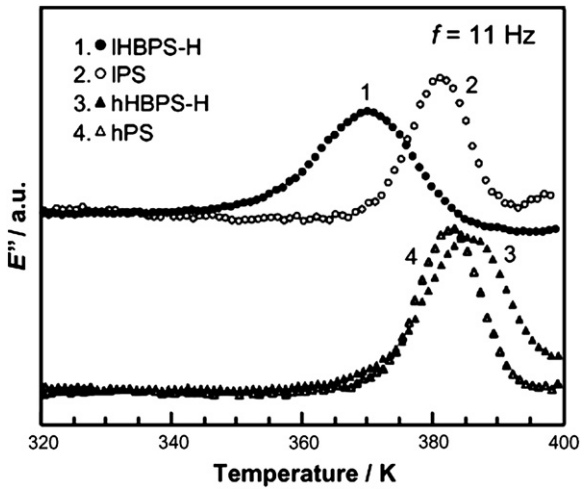

Fig. 8. Temperature dependence of dynamic loss modulus for HBPS-Hs and linear PSs at 11 Hz.

original sample and the product. The ΔT_g increased with annealing time in both cases. The time evolution of ΔT_g was much faster with photo-irradiation than in its absence. This is because the cross-linking proceeds faster under UV irradiation due to the accelerated formation of radicals from DC groups. Panel (b) of Fig. 7 shows the normalized IR spectra for neat HBPS–DC, HBPS–DC annealed for 240 min at 423 K without UV irradiation, and HBPS–DC annealed for 6, 30 and 240 min at 423 K with UV irradiation, corresponding to the locations marked with arrows in Fig. 7(a). Since all the spectra were normalized with the internal standard peak at 1510 cm^{-1} [51–53], they can be directly compared to one another. A decrease in the intensity of the absorption peaks at 1485 cm^{-1}, which corresponds to the C–N stretching vibration of DC groups, reflects the progress of cross-linking process. The order of the heights of the absorption peaks was the inverse of the order for ΔT_g. Thus, it is clear that the presence of cross-linking makes T_g higher. The extent of the T_g increment induced by cross-linking seems to be reasonable after taking into account simulation results as well as results from other polymeric systems using cross-linkers [58].

3.5. Glass transition dynamics

So far, the glass transition temperatures of HBPS-H and HBPS–DC were discussed. Now, we examine the glass transition dynamics of HBPS-H by DMA. Due to the necessity of a relatively large amount of samples for these measurements, we prepared the specimens using samples that had not been fractionated. Fig. 8 shows the temperature dependence of the dynamic loss modulus (E'') for films of HBPS-H with low and high M_w, such as *l*HBPS-H and *h*HBPS-H. The data for the corresponding linear PSs are also presented. For the sake of clarity, each data set was only plotted at a measurement frequency (f) of 11 Hz. In all cases, the α_a-absorption peak arisen from the segmental motion was clearly observed, and the peak position systematically shifted depending on the measurement frequency (not shown). The absorption peak for *l*HBPS-H appeared at a lower temperature than that of the corresponding PS by approximately 10 K. On the other hand, the α_a-relaxation process for *h*HBPS-H appeared to a higher temperature than that for the corresponding linear PS. These results are entirely consistent with those found by DSC presented in Fig. 2.

Fig. 9(a) shows the relation between temperature (T) and relaxation time (τ) for the α_a-process in *l*HBPS-H, *h*HBPS-H and PS films. The τ value at T was simply calculated by $1/(2\pi f)$ at which E'' was maximized. The T–τ relation for polymers is generally expressed by the Vogel–Fulcher (VF) equation [59,60].

$$\tau = \tau_0 \exp\{B/(T - T_v)\} \quad (2)$$

Here, T_v is Vogel temperature, at which viscosity diverges to infinity; it is generally equal to T_g-50. The parameters τ_0 and B are characteristic time related to molecular vibration, and activation temperature, respectively. Using a τ_0 value of 10^{-14} s [61], and with B and T_v as fitting parameters, equation (2) produced the solid curves, which were in good agreement with the experimental results. Table 3 summarizes the fitting parameters for the VF analysis. In the case of linear PS, both the B and T_v values so obtained were consistent with those reported values by other experimental techniques such as dielectric relaxation spectroscopy (DRS) [62]. In contrast, B for HBPS-H somewhat deviated from that for PS. In addition, the T_v value for HBPS-H was slightly lower than T_g-50 K, especially for *l*HBPS-H. These infer that the glass transition dynamics of HBPS-H is essentially different from that of linear PS.

It is generally accepted that the characteristics of glass-forming materials can be classified by a fragility index (m), which is closely related to the slowing down of the segmental dynamics as the temperature approaches the T_g [63,64]. If a substance is a strong liquid, the relation of temperature to segmental relaxation time shows an Arrhenius behavior. This means that the index becomes smaller. However, when a substance is a polymeric material in which the segmental motion is cooperative, its nature is fragile, resulting in a higher value of m. In these experiments, the m value can be extracted from the tangential line at $\tau = 100$ s, which closely corresponds to the T_g [63–65], using:

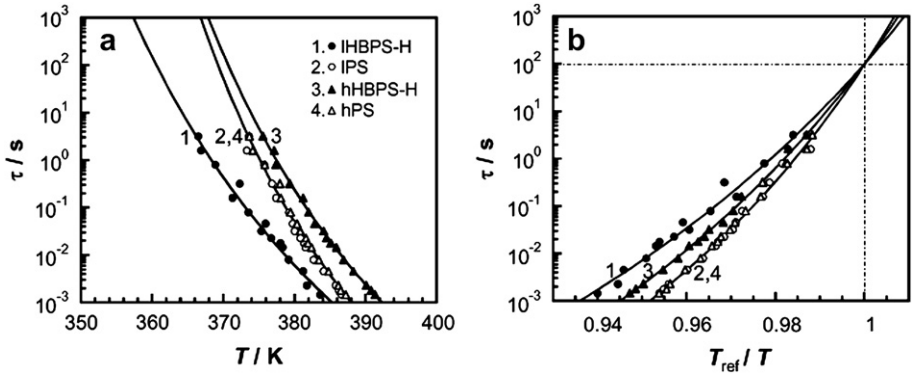

Fig. 9. (a) Temperature dependence of relaxation time for the α_a-process in HBPS-H and PS films. (b) Relation between reciprocal temperature and relaxation time. The abscissa is normalized by the reference temperature, at which τ is equal to 100 s. The solid curves denote the best fit predicted by the Vogel–Fulcher equation using parameters shown in Table 3.

Table 3
Fitting parameters of VF analysis for HBPS-H and linear PS films.

Sample	B/K	T_v/K	m
*l*HBPS-H	2000	306	106
*l*PS	1510	328	144
*h*HBPS-H	1750	323	125
*h*PS	1520	328	144

$$m = \mathrm{d}\log(\tau)/\mathrm{d}(T_g/T) \quad (3)$$

To estimate m, τ was re-plotted against the reciprocal absolute temperature ($1/T$), which was normalized by the reference temperature (T_{ref}), defined at $\tau = 100$ s in Fig. 9(a). Fig. 9(b) shows the results, a so-called Angell plot [63,64]. This plot clearly shows that the $(T_{ref}/T)-\tau$ relations for two linear PSs with different M_w were superimposed, meaning that the m values were almost the same for both. The m values for *l*PS and *h*PS were equal to be 144, which are in quantitative agreement with reported values [65]. On the other hand, the $(T_{ref}/T)-\tau$ curves for *l*HBPS-H and *h*HBPS-H did not overlap. In this case, the m values for *l*HBPS-H and *h*HBPS-H were 106 and 125, respectively, being smaller than those for linear PSs. It is interesting to note that, although the T_gs for *l*HBPS-H and *h*HBPS-H were, respectively, lower and higher, than those of the corresponding linear components, the m values for both *l*HBPS-H and *h*HBPS-H were always smaller than that of PS with an equivalent M_w. Invoking the idea that a smaller m means a less cooperative segmental motion [66], we conclude that the segmental motion for HBPS-H is less cooperative than that for the corresponding linear PS, probably due to a lack of intermolecular entanglements. This interpretation is similar to that invoked for the segmental dynamics for linear PS with an M_w being smaller than the entanglement limit [65,67].

Kwak et al. reported that hyper-branched poly(ether ketone) was more fragile than the corresponding linear component [37]. This was because the HBP was denser than the linear component [37], meaning that their m value results incorporated not only a branching effect but also a packing effect. On the contrary, the density of our HBPS-H measured by a conventional pycnometry was 1.046, which is comparable to or less than that of linear PS. Hence, it is likely that their reasoning for their fragility claim is not applicable in our case. In addition, Roland et al. and Mano et al. studied the effect of cross-linking on m using polymers gelated by cross-linkers, and found that the m value increased with an increasing number density of cross-linking points [68–70]. This seems to be quite reasonable; given that they mixed a cross-linking agent into the polymerization system, the network structure should be well developed over the usual polymer dimensions. In contrast, the only network structure in our HBPS-H is within a molecule, resulting in a lack of intermolecular entanglements. Thus, it is conceivable that the size difference in the network structures caused an opposite cross-linking effect on the m value in the observations of Roland et al. and Mano et al. from that observed in this work. Furthermore, it should be always kept in mind that HBPS-H may not truly resemble polystyrene. Introducing hyper-branching structure into a polymeric molecule generates new structural features that can alter the chemistry. Thus, as shown in Figs. 1 and 4, using DTCS as the monomer to make HBPS introduces C–C and/or C–C–C units between phenyl rings, rather than the single methylene link in PS. Thus, for the moment, we are not able to exclude the possibility that the discrepancy in the glass transition behavior between HBPS and linear PS is controlled not only by branching and end group effects, but also differences in chemical structure.

According to Angell's argument, dynamic fragility should be associated with the heat capacity change at T_g, namely ΔC_p. This notion claims that there is a positive correlation between m and ΔC_p, as demonstrated for nonpolymeric glass-forming liquids [71]. Huang and McKenna extended this idea, and proposed that there is a fragility dilemma in glass-forming liquids [72]. They classified m vs. ΔC_p relations into three regimes, depending on how dynamic fragility correlates with the equivalent thermodynamic property: polymeric glasses with a negative correlation, organic small molecules with no correlation, and inorganic glass-formers with a positive one. To discuss further the effect of architecture on the segmental dynamics, the relationship between dynamic and thermodynamic fragilities for HBPS is directly compared with that for PS. Fig. 10 shows the relation between ΔC_p and m values for HBPS and PS. The data for linear PS reported by Roland et al. [65] are also plotted and exhibit a negative correlation between ΔC_p and m. Our data for linear PS followed similar typical behavior for polymeric glasses [72]. On the other hand, in the case of HBPS, no clear correlation seems to exist between ΔC_p and m. This may be a sign that HBPS can be regarded as small organic molecules rather than entangled polymeric materials [72]. This speculation is quite consistent with our experience that self-supporting films of HBPS cannot be prepared. Further support for this supposition comes from the consideration that a hyper-branching structure prevents the formation of entanglements between neighboring molecules due to the presence of shorter chains between branching points as well as intramolecular cyclic portions. Such a less entangled system would reduce the amount of cooperativity in the segmental motion, as indicated by the experimental data in Fig. 9. Again, it should be always kept in mind that the discrepancy of glass transition dynamics between HBPS and linear PS may be controlled by not simply the effect of its unique architecture, but also by the differences in chemical structure.

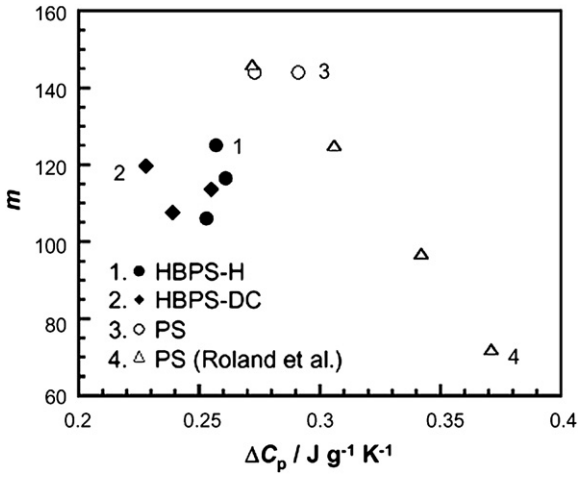

Fig. 10. Relationship between heat capacity change at T_g and fragility index for HBPS and PS. Data reported by Roland et al. are also plotted in the figure.

4. Conclusions

If hyper-branched polystyrenes follow the general trend observed for glass transitions, the T_g of HBPS should be lower than that of the corresponding linear PS due to the dominant effects of chain end portions. In fact, the bulk glass transition temperature of HBPS–DC was lower than that of HBPS-H at a given M_w. However, two different fractions of HBPS-H with an equivalent M_w showed T_g values that were respectively higher and lower than that of the corresponding linear PS. One possible reason for the T_g being higher than that of the linear PS with a comparable M_w is if a cyclic structure is well

developed in the hyper-branched molecule. A fragility analysis implies that the segmental motion of HBPS was always less cooperative than that of linear PS. Since a HBPS molecule possesses shorter segments between branching points, as well as intramolecular cyclic portions, unlike a linear PS with a higher M_w, intermolecular entanglements would not form among HBPS molecules. Thus, we conclude that the glass transition dynamics of hyper-branched polymers is controlled by not just chain end and branching effects, but also the presence of intramolecular cyclization.

Acknowledgements

We would like to express our deep appreciation of fruitful discussions with Prof. K. Fukao (Ritsumeikan Univ.), Prof. K. Saito (Univ. of Tsukuba), Prof. A. Takahara, Dr. M. Kobayashi, Ms. Y. Mizutani (Kyushu Univ.), and Dr. M. Miyamoto, Mr. K. Odoi, Mr. A. Tanaka, Dr. K. Yasui, and Dr. O. Hirata (Nissan Chemical Ind. Ltd.). This research was partly supported by the Grant-in-Aids for Young Scientists A (No. 21685013), for Science Research in a Priority Area "Soft Matter Physics" (No. 21015022) and for the Global COE Program, "Science for Future Molecular Systems" from the Ministry of Education, Culture, Sports, Science and Technology, Japan. This research was also supported in part by the Industrial Technology Research Grant Program in 2006 from the New Energy and Industrial Technology Development Organization (NEDO) of Japan.

References

[1] Tomalia DA, Naylor AM, Goddard III WA. Angew Chem Int Ed Engl 1990; 29:138–75.
[2] Fréchet JMJ. Science 1994;263:1710–5.
[3] Aoi K, Itoh K, Okada M. Macromolecules 1995;28:5391–3.
[4] Jiang DL, Aida T. Nature 1997;388:454–6.
[5] Matthews OA, Shipway AN, Stoddart JF. Prog Polym Sci 1998;23:1–56.
[6] Fischer M, Vogtle F. Angew Chem Int Ed 1999;38:885–905.
[7] Bosman AW, Janssen HM, Meijer EW. Chem Rev 1999;99:1665–88.
[8] Inoue K. Prog Polym Sci 2000;25:453–571.
[9] Vögtle F, Gestermann S, Hesse R, Schwierz H, Windisch B. Prog Polym Sci 2000;25:987–1041.
[10] Schluter AD, Rabe JP. Angew Chem Int Ed 2000;39:864–83.
[11] Cagin T, Wang GF, Martin R, Breen N, Goddard WA. Nanotechnology 2000; 11:77–84.
[12] Grayson SM, Fréchet JMJ. Chem Rev 2001;101:3819–67.
[13] Hecht S, Fréchet JMJ. Angew Chem Int Ed 2001;40:74–91.
[14] Yamamoto K, Higuchi M, Shiki S, Tsuruta M, Chiba H. Nature 2002;415:509–11.
[15] Majoros IJ, Myc A, Thomas T, Mehta CB, Baker JR. Biomacromolecules 2006; 7:572–9.
[16] (a) Voit BI. Acta Polym 1995;46:87–99;
(b) Voit BI. J Polym Sci Part A Polym Chem 2005;43:2679–99.
[17] Kim YH. J Polym Sci Part A Polym Chem 1998;36:1685–98.
[18] Jikei M, Kakimoto M. Prog Polym Sci 2001;26:1233–85.
[19] Miller TM, Neenan TX, Zayas R, Bair HE. J Am Chem Soc 1992;114:1018–25.
[20] Morikawa A, Kakimoto M, Imai Y. Macromolecules 1992;25:3247–53.
[21] (a) Wooley KL, Hawker CJ, Pochan JM, Fréchet JMJ. Macromolecules 1993; 26:1514–9;
(b) Wooley KL, Fréchet JMJ, Hawker CJ. Polymer 1994;35:4489–95.
[22] De Brabander-van den Berg EMM, Meijer EW. Angew Chem Int Ed Engl 1993;32:1308–11.
[23] Stutz H. J Polym Sci Part B Polym Phys 1995;33:333–40.
[24] Emran SK, Newkome GR, Weis CD, Harmon JP. J Polym Sci Part B Polym Phys 1999;37:2025–38.
[25] (a) Kim YH, Webster OW. Macromolecules 1992;25:5561–72;
(b) Kim YH, Beckerbauer R. Macromolecules 1994;27:1968–71.
[26] Turner SR, Voit BI, Mourey TH. Macromolecules 1993;26:4617–23.
[27] Chu F, Hawker CJ. Polym Bull 1993;30:265–72.
[28] (a) Malmström E, Johansson M, Hult A. Macromolecules 1995;28:1698–703;
(b) Malmström E, Johansson M, Hult A. Macromol Chem Phys 1996;197: 3199–207;
(c) Malmström E, Hult A, Grdde UW, Liu F, Boyd RH. Polymer 1997;38:4873–9.
[29] (a) Kumar A, Ramakrishnan S. Macromolecules 1996;29:2524–30;
(b) Behera GC, Ramakrishnan S. Macromolecules 2004;37:9814–20.
[30] Morikawa A. Macromolecules 1998;31:5999–6009.
[31] (a) Yang G, Jikei M, Kakimoto M. Macromolecules 1999;32:2215–20;
(b) Hao J, Jikei M, Kakimoto M. Macromolecules 2003;36:3519–28.
[32] (a) Shu CF, Leu CM, Huang FY. Polymer 1999;40:6591–6;
(b) Gong ZH, Leu CM, Wu FI, Shu CF. Macromolecules 2000;33:8527–33;
(c) Wu FI, Shu CF. J Polym Sci Part A Polym Chem 2001;39:2536–46.
[33] Sunder A, Bauer T, Mülhaupt R, Frey H. Macromolecules 2000;33:1330–7.
[34] (a) Knauss DM, AI-Muallem HA, Huang T, Wu DT. Macromolecules 2000;33: 3557–68;
(b) Knauss DM, AI-Muallem HA. J Polym Sci Part A Polym Chem 2000;38: 4289–98.
[35] Schmaljohann D, Häußler L, Pötschke P, Voit BI, Loontjens TJA. Macromol Chem Phys 2000;201:49–57.
[36] Parker D, Feast WJ. Macromolecules 2001;34:2048–59.
[37] Ahn DU, Kwak SY. Macromol Mater Eng 2001;286:17–25.
[38] Orlicki JA, Thompson JL, Markoski LJ, Sill KN, Moore JS. J Polym Sci Part A Polym Chem 2002;40:936–46.
[39] Lee JS, Quirk RP, Foster MD. Macromolecules 2005;38:5381–92.
[40] Gong W, Mai Y, Zhou Y, Qi N, Wang B, Yan D. Macromolecules 2005;38:9644–9.
[41] Flory PJ. J Am Chem Soc 1952;74:2718–23.
[42] Ishizu K, Mori A. Macromol Rapid Commun 2000;21:665–8.
[43] Available at: http://polymer.nims.go.jp/PoLyInfo/prop-est.html.
[44] van Krevelen DW. Properties of polymers. 3rd ed. Elsevier; 1990.
[45] Hawker CJ, Lee R, Fréchet JMJ. J Am Chem Soc 1991;113:4583–8.
[46] Hölter D, Burgath A, Frey H. Acta Polym 1997;48:30–5.
[47] The degree of branching (DB) is generally defined as (branching and terminal units)/(branching, linear and terminal units). In the case of AB_2 type hyper-branched system, DB is formulated as $2D/(2D+L)$, where D and L are the numbers of branching and linear units [46], respectively, provided that the number of terminus is given by $D+1$ under the assumption of $D \gg 1$. We here simplify the sequence of HBPS as a combination of styrene-like units and phenylene-like ones, which corresponds to a linear component and a branching one, respectively. When the fractional amount of styrene-like unit is x, L and D can be expressed as $(n-2)\cdot x$ and $(n-2)\cdot(1-x)$, respectively, where n is the degree of polymerization. Thus, the DB value can be simply given by n and x. In the case of HBPS–DC, x could be estimated on the basis of the intensity ratio of usual methylene protons at 1–2.4 ppm to methylene ones connected to a DC group at 4.7 ppm. The DB values for HBPS–DC with a lower and higher M_w were 0.219 ± 0.071 and 0.206 ± 0.130, respectively, being smaller than the ideal value of 0.50 [46]. These values are comparable to the reported value for the same polymerization system estimated by a kinetic approach [48]. Unfortunately, the above-mentioned method could not be simply applied to HBPS-H, because the chemical shift of all protons in methyne, methylene, and methyl units directly connected to phenyl rings in ^{1}H NMR measurement could not be distinguished among one another. Considering the reduction process from HBPS–DC to HBPS-H, it seems reasonable to postulate that the DB value is not so altered before and after the reduction reaction. The HBPS–DC with a lower and higher M_w, which the DB values were obtained, became *l*HBPS-H and *h*HBPS-H after the reduction reaction. Thus, we believe that the DB values for *l*HBPS-H and *h*HBPS-H are 0.219 ± 0.071 and 0.206 ± 0.130, respectively. The slight difference might be due to the consumption of end groups, resulting from the intramolecular cyclization.
[48] Ishizu K, Ohta Y, Kawaguchi S. J Appl Polym Sci 2005;96:1810–5.
[49] Akabori K, Tanaka K, Nagamura T, Takahara A, Kajiyama T. Macromolecules 2005;38:9735–41.
[50] Fox TG, Flory PJ. J Polym Sci 1954;14:315–9.
[51] Yang JC, Jablonsky MJ, Mays JW. Polymer 2002;43:5125–32.
[52] Brijmohan SB, Swier S, Weiss RA, Shaw MT. Ind Eng Chem Res 2005;44:8039–45.
[53] Meng G, Li A, Yang W, Liu F, Yang X, Zhang Q. Eur Polym J 2007;43:2732–7.
[54] Manav N, Mishra AK, Kaushiki NK. Spectrochim Acta Part A 2007;67:995–1002.
[55] Ishizu K, Ohta Y, Kawauchi S. Macromolecules 2002;35:3781–4.
[56] The IR and ^{1}H NMR spectra for the fractionated HBPS were almost the same as those for the original one. This indicates that the primary structure of a fractionated sample should be comparable to that of a parent one. Thus, it is expected that the difference of the hydrodynamic size corresponds to the molecular weight difference.
[57] Based on the IR and ^{1}H NMR results of HBPS-H, the numbers of methyl terminus in the model structures for *l*HBPS-H and *h*HBPS-H were set to be 4 and 2, respectively. In addition, the number ratio of C–C–C sequences to C–C ones was fixed to 6:1 for *l*HBPS-H and 4:3 for *h*HBPS-H.
[58] Sasaki T, Uchida T, Sakurai K. J Polym Sci Part B Polym Phys 2006;44:1958–66.
[59] Vogel H. Phys Z 1921;22:645–6.
[60] Fulcher GS. J Am Ceram Soc 1925;8:339–55.
[61] Ngai KL, Rizos AK. Mater Res Soc Symp Proc 1997;455:147.
[62] Fukao K, Miyamoto Y. Phys Rev E 2001;64:011803.
[63] Böehmer R, Ngai KL, Angell CA, Plazek DJ. J Chem Phys 1993;99:4201.
[64] Angell CA. Science 1995;267:1924–35.
[65] Santangelo PG, Roland CM. Macromolecules 1998;31:4581–5.
[66] Plazek DJ, Ngai KL. Macromolecules 1991;24:1222–4.
[67] Rozos AK, Ngai KL. Macromolecules 1998;31:6217–25.
[68] Roland CM, Santangelo PG, Antonietti M, Neese M. Macromolecules 1999;32:2283–7.
[69] Robertson CG, Santangelo PG, Roland CM. J Non-Cryst Solids 2000;275:153–9.
[70] Alves NM, Gómez Ribelles JL, Gómez Tejedor JA, Mano JF. Macromolecules 2004;37:3735–44.
[71] Wang LM, Angell CA, Richert R. J Chem Phys 2006;125:074505.
[72] Huang D, McKenna GB. J Chem Phys 2001;114:5621–30.